Materials Science & Engineering B xxx (xxxx) 115815

Contents lists available at ScienceDirect

Materials Science & Engineering B

journal homepage: www.elsevier.com/locate/mseb

Changing the polarization and mechanical response of flexible PVDF-nickel ferrite films with nickel ferrite additives

Bedanga Sapkota [a], Alix Martin [a], Haidong Lu [b], Rifat Mahbub [c], Zahra Ahmadi [c], Soodabeh Azadehranjbar [c], Esha Mishra [b], Jeffrey E. Shield [c, d], Shaik Jeelani [a], Vijaya Rangari [a, *]

[a] Department of Material Science and Engineering, Tuskegee University, Tuskegee, AL 36088 USA
[b] Department of Physics and Astronomy, University of Nebraska, Lincoln, Nebraska 68588, USA
[c] Department of Mechanical & Materials Engineering, University of Nebraska, Lincoln, Nebraska 68588, USA
[d] Nebraska Center for Materials and Nanoscience, University of Nebraska, Lincoln, Nebraska 68588, USA

ARTICLE INFO

Keywords:
Nickel ferrite
PVDF
Polymer film
Nanocomposite
Ferroelectric
Magnetization

ABSTRACT

Polymer-based flexible nanocomposite films, of nickel ferrite nanoparticles in a polyvinylidene fluoride (PVDF) polymer matrix, were fabricated using a blade coating technique. A two-step process is used to prepare nanocomposite films. The first process involves the synthesis of nickel ferrite ($NiFe_2O_4$) nanoparticles using sonochemical method, and then incorporation of various weight percentage (5, 10, 20, and 30%) of nickel ferrite nanoparticles into the PVDF to form polymer nanocomposites. Nickel ferrite nanoparticles demonstrated a magnetization of 37.3 emu/g at magnetic field of 5 kOe while 30% Nickel-ferrite-PVDF nanocomposite shows 23.8 emu/g. Finally, the ferroelectric and local polarization switching properties of pure PVDF and nanocomposite films were investigated via piezoresponse force microscopy (PFM) measurements. The pure PVDF film demonstrates a negative piezoelectric coefficient from the PFM hysteresis loop measurement whereas the nanocomposite film shows a positive piezoelectric coefficient with an opposite PFM signal.

1. Introduction

Commonly used multiferroic materials are ceramic and polymer-based composites. Ceramic-based composites are less favored from the application point of view due to lack of flexibility, low processability and high leakage current density.[1] Polymer-based composites overcome these limitations and have demonstrated relatively stronger electromagnetic properties, low dielectric constants and dielectric loss.[2–5] In addition, these materials offer unique advantages over ceramic such as they can be fabricated into different shapes such as thin films and molded structures as well as can be formed easily on to the curved surfaces. Thus, making them suitable for applications such as sensors, transducer, actuators, and miniature antennas.[6–11] Magnetoelectric coupling in such polymer-based composite systems can be tuned by varying different parameters such as the weight (%) of the components and composite architecture.[12,13] (SeeScheme 1.).

Polyvinylidene fluoride (PVDF) is a semi-crystalline polymer that can crystallize in four different crystalline phases known as α, β, γ, and δ.[14] The existence of these phases depends on the processing conditions or synthesis processes. The α and β phases are the most interesting ones for technological applications and are widely studied. The α phase is known as the non-polar stable phase and the β phase is known as the polar phase. In the β phase all-trans planar zig–zag conformation results in a non-zero dipole moment, resulting in remarkable ferroelectric properties.[15] β phase is the only one that possesses a spontaneous polarization, and therefore piezoelectricity.[16] Because of multifunctional properties such as ferroelectric, pyroelectric, and piezoelectric, PVDF can be used for sensors, actuators, batteries, nanogenerator, and in the biomedical field.[17–20].

To introduce magnetoelectric coupling in ferroelectric PVDF, spinal ferrites AFe_2O_4 (A = Ni, Co, Zn, Cd, Mn, Cu, Mg) with good magnetization are preferred.[2] In this study, sonochemically synthesized nickel ferrite nanoparticles were infused into a ferroelectric PVDF polymer, such that the coupling and synergetic interaction between ferromagnetic NiFe2O4 and ferroelectric PVDF could lead to the development of magnetoelectric nanocomposites with possible numerous technological applications. Furthermore, with the addition of such nanofillers in the polymer matrix, thermal properties may be changed or improved, which can in turn modify the application range of the materials. For such, the understanding of how thermal/magnetic/electric properties

* Corresponding author.
E-mail address: vrangari@tuskegee.edu (V. Rangari).

https://doi.org/10.1016/j.mseb.2022.115815
Received 20 August 2021; Accepted 6 June 2022
0921-5107/© 20XX

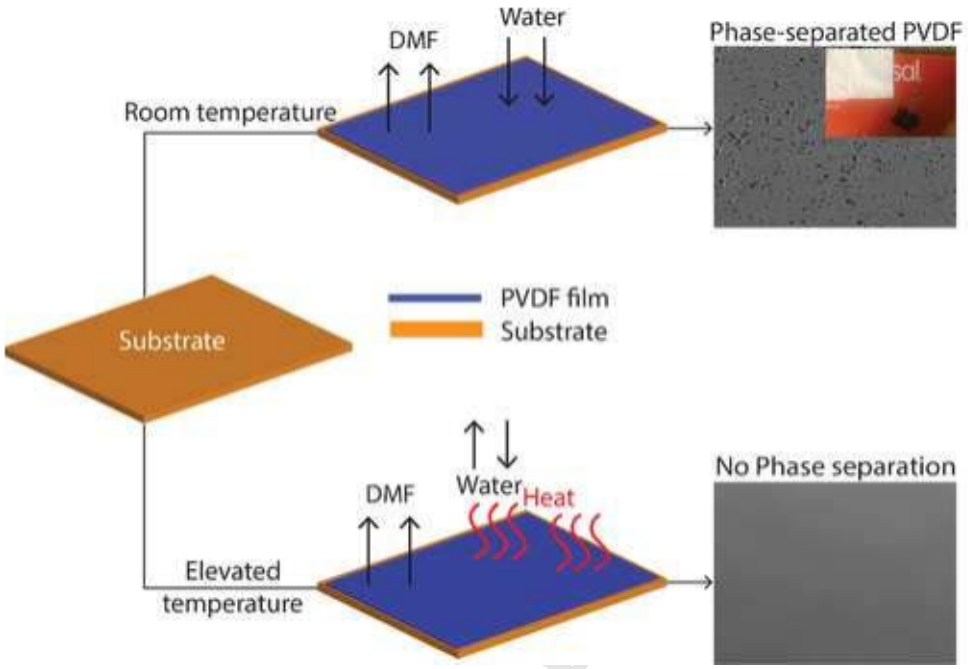

Scheme 1. Graphical depiction of the fabrication process for phase-separated porous PVDF film and void-free smooth film. Inset: Photograph of phase-separated opaque PVDF film (white color).

are changed due the physical and chemical interaction between nanoparticles and polymer is essential. Additionally, by addressing how nanoparticles induce variations in the thermal properties and thermal degradation of polymers, valuable information on the nature of the particle-polymer interactions can be understood.

Earlier studies have reported a number of preparation methods, for PVDF-based nanocomposites films such as PVDF-$BiFeO_3$,[21] PVDF-$CoFe_2O_4$,[22,23] and PVDF-$NiFe_2O_4$,[24,25] using either a solution casting, or hot press, or a combination of both to improve the magneto-electric coupling. In those studies, enhancements in magnetoelectric coupling and dielectric constant with the increase in filler nanoparticles were reported. However, because of stochastic nature of the processes, it is very difficult to prepare large films and control thickness using those methods. Additionally, nanocomposite films often encountered with voids and aggregated ferrite particles in the polymer matrix. In contrast, microelectronic applications require thinner and pinhole-free films to operate at low-voltage and to prevent from electrical shorts, respectively. To address aforementioned issues, spin-coating was used to prepare the PVDF film. However, an inhomogeneous film was observed, which was also found to suffer from an opaque or cloudy nature of PVDF film (data are not shown here). Herein, we report a straightforward route for the fabrication of large, flexible, and highly smooth pure PVDF and nickel-ferrite-PVDF nanocomposites films using doctor blade technique, wherein thickness of the films can be controlled using thickness adjustable film coater or casting blade. Additionally, using this technique speed of coating and temperature of substrate can be controlled in between 20 °C and 110 °C. We observe that voids present in the films due to exchange of solvent (DMF) and non-solvent (water vapor from ambient humidified air) can be avoided by raising the substrate temperature at or above 95 °C. To our knowledge, this is the first report for the fabrication of large flexible mangeto-electric film with controlled thickness and microstructures.

2. Experimental

2.1. Materials

All chemicals used in the reaction were of analytical grade and were purchased from Sigma-Aldrich. PVDF $(-CH_2-CF_2-)_n$ with an of average molecular weight of 180, 000 by gel permeation chromatography (GPC) and N,N-dimethylformamide (DMF) (C_3H_7NO) were used for the fabrication of the films. Nickel nitrate and iron acetate precursors used to synthesize nickel ferrite nanoparticles were purchased from Sigma-Aldrich.

2.2. Synthesis of nickel ferrite nanoparticles

NiFe2O4 nanoparticles were synthesized from nickel nitrate and iron acetate precursors with the assistance of ultrasound irradiation. A reaction mixture of nickel nitrate (0.5 g) and iron acetate (1 g) in 60 mL of solvent (50 mL of water and 10 mL of DMF) was prepared and sonicated for a 2-h by employing a probe sonicator (Model PRO-500, 20 kHz, 500 W). The probe is made of high-grade titanium with a diameter of 13 mm. It was driven at a frequency of 20 kHz and operated at 62% amplitude. Cavitation produced by intense ultrasonic waves was strong enough to drive reactions like oxidation, reduction, decomposition, hydrolysis, and dissolution.[26] A black solid precipitate was obtained after a 2-h irradiation and was separated by centrifugation. The resulting precipitate was dried overnight in an oven at 80 °C and the final product was calcined at 600 °C for a 5 h.

2.3. Fabrication of polymer nanocomposite films

PVDF was dissolved in DMF as PVDF crystallizes in the β phase when the films are fabricated using DMF as the solvent. A 15 wt% of PVDF homogeneous solution was prepared by continuously heating and stirring PVDF pellets in DMF at 80 °C. It is noted that at low temperature very small crystallites still present in the solution, due to partial dissolution or refolding of the polymer chain, which could act as nuclei when the solution is recrystallized. We observe that only by raising the temperature complete dissolution of PVDF can be achieved but not by

longer dissolution time. Once complete dissolution of the PVDF was achieved, an appropriate amount of nickel ferrite was added to the solution to prepare a series of various content (0, 5, 10, 20 and 30 wt%) of nickel ferrite in the solution while magnetically stirring for 30 min. The reaction solutions were then sonicated for at least a 1-h to attain a uniform distribution of nickel ferrite nanoparticles in the polymer solution. The homogeneous dispersion thus obtained was used to prepare films using a film coater. The PVDF films were prepared at room temperature and at various substrate temperature up to 95 °C. At 95 °C, we observe smooth and void free films; thus, all the nanocomposite films were prepared at 95 °C. As-fabricated pure PVDF and nanocomposites films were then heated at 135 °C for a 1-h to facilitate the formation of β-phase in the PVDF and PVDF–nickel ferrite nanocomposites. It was then allowed to cool down to room temperature, forming pure PVDF and PVDF-nickel ferrite nanocomposite films, which were then stored for characterization and thin film analysis.

2.4. Characterization techniques

X-ray diffraction (XRD) patterns of the synthesized nickel ferrite nanoparticles and nanocomposite films were recorded using an X-ray diffractometer (Rigaku) with a Cu-Kα line (wavelength 1.54 Å). The accelerating voltage and current was set to 40 kV and 30 mA, respectively. The XRD data were analyzed using MDI JADE software. Transmission electron microscopy (HRTEM, JEOL) analysis was performed to estimate the particle size and shape of the prepared nickel ferrite nanopowder. FTIR spectra of the pure PVDF and nanocomposite films were recorded using attenuated total reflectance-FTIR (Nicolet, Nexus model 670/870) at room temperature. The spectra were recorded between 600 and 1000 cm^{-1} with a resolution of 4 cm^{-1} and total scans were 32 per sample. Surface morphology of the pure PVDF and nanocomposites films were obtained using field emission scanning electron microscope (FESEM, JEOL). The thermal properties of pure PVDF and nanocomposites were evaluated using a thermal gravimetric analyzer (TGA Q500, TA instrument). Samples were analyzed under a nitrogen atmosphere to prevent from temperature related oxidative process and were carried out from 30 to 1000 °C at the constant heating rate of 10 °C/min The magnetic properties of the nickel ferrite nanoparticles and polymer nanocomposites were studied using superconducting quantum interference device (SQUID) at room temperature. To estimate the magnetization of nanocomposite, the obtained magnetization value is normalized to the weight of the composite, and not the weight of the nickel ferrite nanoparticles.

3. Results and discussion

3.1. Structural characterization

X-ray diffraction patterns of nickel ferrite nanoparticles, pure PVDF film, and the nanocomposite films are shown in Fig. 1a-b. As shown in Fig. 1a, the PVDF film has distinct diffraction peaks at 18.84°, 20.40°, 36.62°, and 39.26°. The strong peaks at 18.84° and 20.40° correspond to the (1 1 0) and (2 0 0) planes of the β phase. The observed strong β phase of the PVDF film can be attributed to the preferential crystallization of PVDF while using DMF as the solvent.[27] The low intensity peaks at 36.62° and 39.26° are attributed to the γ (2 0 0) and α (0 0 2) phases of PVDF.[25] This result suggests that the plain PVDF film possesses a combination of α, β, and γ crystalline polymorphs with a relatively higher quantity of the ferroelectric β phase. Fig. 1b shows the diffraction pattern of as-synthesized nickel ferrite nanoparticles. The typical reflections of the {1 1 1}, {2 2 0}, {3 1 1}, {2 2 2}, {4 0 0}, {4 2 2}, {5 1 1}, and {4 4 0} planes were observed, which indicate the cubic spinel structure of the highly crystalline nickel ferrite nanoparticles. All the observed peaks match well with the standard JCPDS 86–2267. The crystallite size (L) of nickel ferrite nanoparticles was calculated from the most intense diffraction peak i.e. (3 1 1) plane by using Debye-Scherrer equation:

$$L = \frac{K\lambda}{\beta cos\theta}$$

where λ is the wavelength of the X-ray radiation, K is a constant ($K = 0.9$), θ is the Bragg angle and β is the full width at half maxima (FWHM) of the diffraction peak. The crystallite size of the nickel ferrite nanoparticle was calculated to be 9 nm. The x-ray diffraction patterns of the composite films show the characteristic peaks corresponding to β phase of PVDF and NiFe2O4 (Fig. 1b). It is clearly seen that the peaks correspond to nickel ferrite become more intense with the increase in nickel ferrite loading in the PVDF matrix. The α phase of PVDF at 39.26° is presented with the PVDF-5% nickel ferrite and gradually disappeared with the higher loading of nickel ferrite. This implies that nickel ferrite peaks dominated over the peaks of PVDF with the increase in loading of ferrite nanoparticles. The inset shows a photograph of the PVDF thin films prepared at 95 °C substrate temperature, revealing a high optical quality transparent nature of the film. The thickness of the film was

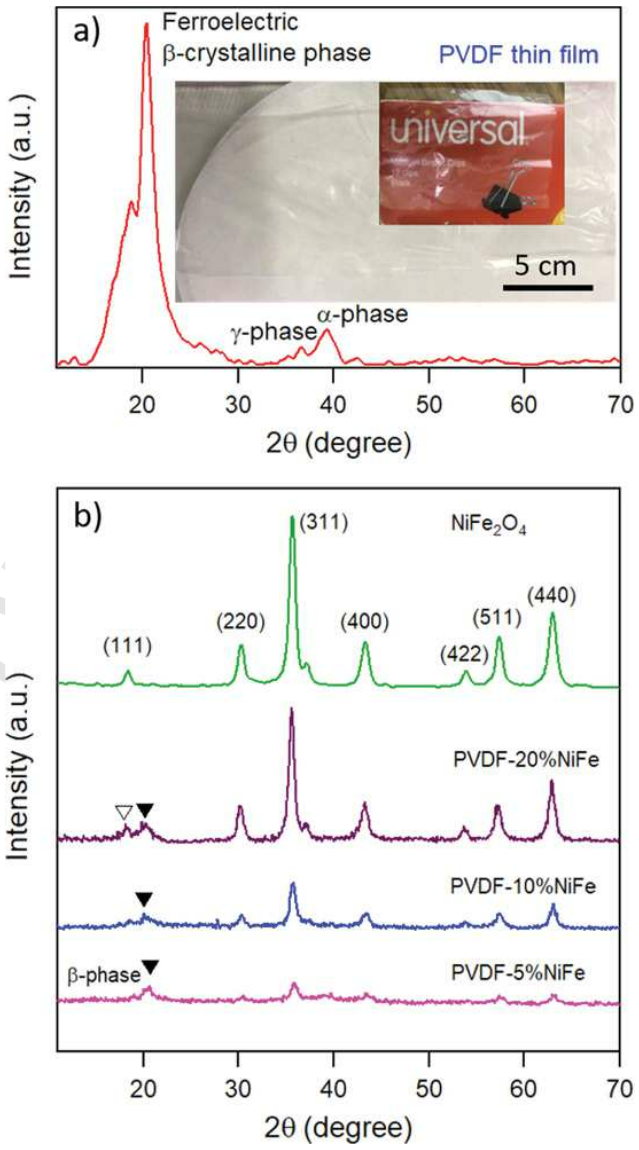

Fig. 1. (a) XRD pattern of pure PVDF thin film and (b) XRD diffraction pattern of nickel ferrite nanoparticle and nanocomposites of PVDF-5% $NiFe_2O_4$, PVDF-10% $NiFe_2O_4$, and PVDF-20% $NiFe_2O_4$. Inset: photograph of PVDF film, showing a transparent nature of the film.

measured using digital screw gauge. The average thickness of the film was found to be (17 ± 2.6) μm, which was obtained by measuring 4 different batches of films in 5 different areas of the films. We observe that speed of coating, temperature of the substrate, and physical properties of solution (viscosity, density) affect the thickness of the film. So, we keep all these parameters constant to control the thickness of the PVDF films.

3.2. Morphology and size analysis of nickel ferrite nanoparticle

SEM and Transmission electron microscopy (TEM) was used to study the surface morphology and size of the nickel ferrite nanoparticles and the results are presented in Fig. 2. The SEM image of the nickel ferrite powder exhibited the formation of aggregates in the form of small spherical grains and interconnected with each other. Similar interconnected behavior of nanopowder is reported previously.[28–32] The TEM image shows that the nickel ferrite nanoparticles are uniformly distributed and spherical in shape. Some separated particles and some moderately aggregated particles could be due to calcination at higher temperature (600 °C). The increase in average particle size and coalescence of the particles due to annealing at higher temperature was also reported previously.[33] The average particle size of the nanoparticles measured from TEM was found to be (18 ± 3.7) nm.

3.3. Phase analysis of neat PVDF and composites

FTIR transmission spectra of the PVDF and nickel ferrite-PVDF nanocomposite films are shown in Fig. 3a. The characteristic transmittance bands corresponding to the α phase (770 and 875 cm^{-1}), β phase (833 cm^{-1}), γ phase (812 cm^{-1}), and β + γ phase (875 cm^{-1}) of the PVDF can be seen.[24] The composite films also demonstrate the strong β and β + γ phase polymorphs at 833 cm^{-1} and 875 cm^{-1} correspond to the C–C–C asymmetrical stretching vibration, CH2 rocking and CF stretching vibration.[14,34] The intensities of the α and β phase polymorphs of PVDF decreases with the increase in amount of NF loading. Although no shift in peaks of the bands is observed with the composite films, the transmission bands at 770 cm^{-1} and 812 cm^{-1} are disappeared with the loading of nanoparticles. This suggests that the incorporation of nickel ferrite nanoparticles influences the crystallization of PVDF. We presume that the ferrite nanoparticle might have constrained the movement of polymer chain by inducing heterogeneous nucleation that could have accelerated the isothermal crystallization of the nanocomposite, leading to influence in crystallization or polymorphs formation.

3.4. Melting peak characterization

DSC curves of pure PVDF and nanocomposite films are shown in Fig. 3b. DSC studies on neat and various wt% of nickel ferrite incorporated

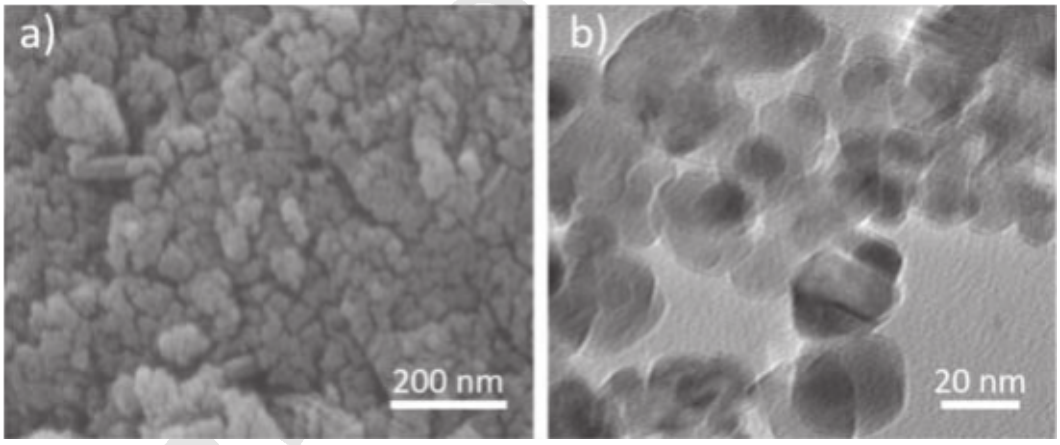

Fig. 2. (a) SEM image of nickel ferrite nanopowder and (b) Bright field TEM micrograph of nickel ferrite nanoparticles prepared using wet chemical approach.

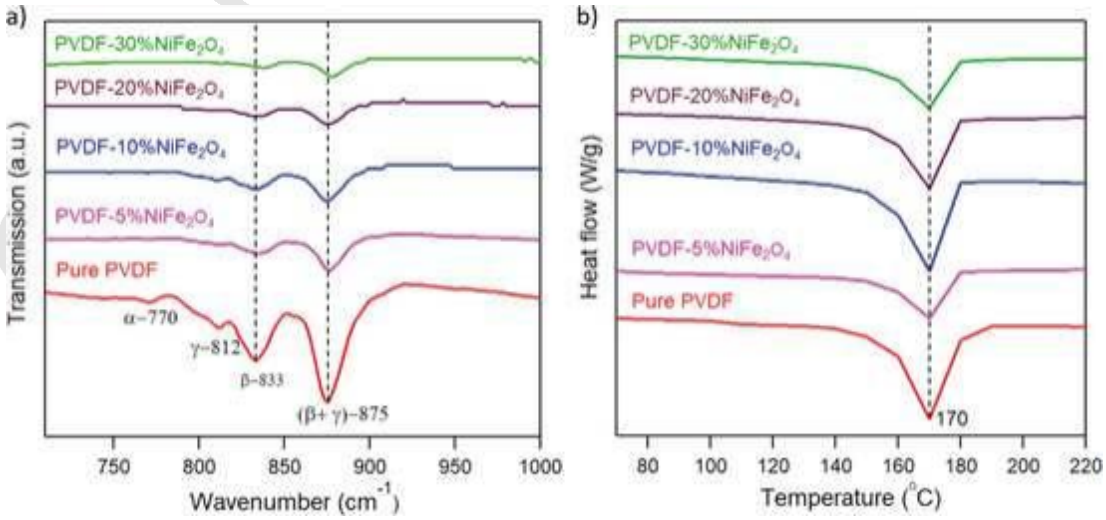

Fig. 3. (a) FT-IR vibrational spectra of the PVDF and nickel ferrite-PVDF composites films. The β crystalline phase at 833 cm^{-1} of PVDF confirms the ferroelectric properties of composites. (b) DSC curve of pure PVDF and nanocomposites films. Nickel ferrite does not have a strong influence on the melting peak.

nanocomposites (PVDF-5% nickel ferrite, PVDF-10% nickel ferrite, PVDF-20% nickel ferrite, and PVDF-30% nickel ferrite) films were performed to study the effect of the nickel ferrite nanoparticles on the melting temperature and the degree of crystallinity of the nanocomposites. Both the pure PVDF and PVDF-NiFc2O4 nanocomposite films show a melting endotherm at 170 °C. The melting temperature of our PVDF film is 11 °C higher than previous report in which a melting endotherm at 159 °C is reported.[24] However, it is within the range of 165–175 °C for PVDF material.[35] There are no significant changes observed, which indicates that $NiFc_2O_4$ does not have a strong influence on the melting temperature of PVDF polymer.

3.5. Melting peak characterization

DSC curves of pure PVDF and nanocomposite films are shown in Fig. 3b. DSC studies on neat and various wt% of nickel ferrite incorporated nanocomposites (PVDF-5% nickel ferrite, PVDF-10% nickel ferrite, PVDF-20% nickel ferrite, and PVDF-30% nickel ferrite) films were performed to study the effect of the nickel ferrite nanoparticles on the melting temperature and the degree of crystallinity of the nanocomposites. Both the pure PVDF and PVDF-NiFe2O4 nanocomposite films show a melting endotherm at 170 °C. The melting temperature of our PVDF film is 11 °C higher than previous report in which a melting endotherm at 159 °C is reported.[24] However, it is within the range of 165–175 °C for PVDF material.[35] There are no significant changes observed, which indicates that $NiFe_2O_4$ does not have a strong influence on the melting temperature of PVDF polymer.

3.6. Surface morphology analysis of PVDF and nanocomposite films

The microstructures of the PVDF film prepared at room temperature and elevated temperature are studied using FE-SEM and are shown in Fig. 4a and Fig. 4b respectively. When the film is prepared at room temperature, a highly rough surface of the PVDF film along with voids due to DMF and water (from humidified air) phase separation can be seen. This unwanted rough surface at room temperature is completely transformed into a very smooth and pore-free surface upon increasing the substrate temperature to 95 °C (see detail in experimental section, Fig. 4b). The inset in Fig. 4a shows the high-resolution image where voids due to phase separation can be seen. It is noted that if the surface of PVDF is highly rough, it becomes brittle and thus cannot be used for flexible electronic applications.[36] On the other hand, the microelectronic applications require thinner and pin-hole free film to operate at low-voltage and to prevent electrical shorts.

The microstructures and distribution of nickel ferrite nanoparticles in the PVDF matrix are shown in Fig. 4c-4e. The distribution of nickel ferrite nanoparticles (white dots in the images) increases with increase in the content of the nanoparticles in the PVDF matrix. It can be seen in the images that, even with the higher percentage of loading, almost uniform distribution of the nickel ferrite nanoparticles in the PVDF matrix was achieved. It is noted that the microstructures of our PVDF films do not show tree-like spherulites as reported previously with solution casting or spin coating method.[25,27,37] This could be due to the predominant ferroelectric β phase in our PVDF films, as evidenced by XRD result (Fig. 1a). The spherulite structures are formed with the α nucleation process of PVDF, and this unfavorable structure is reported to diminish with increased nanoparticle content in PVDF composites due to increased β phase formation. Additionally, unlike previous reports, where significant aggregation of filler particles or formation of voids in PVDF nanocomposite films due to addition of nanoparticles is reported, [2,24] our composite films show uniform distribution of nanoparticles. As shown in Fig. 4c–e, our nanocomposite films are highly smooth and pore-free. Fig. 4f–h show elemental (nickel, iron, and oxygen) maps of PVDF-30 % nickel ferrite nanocomposite film, which confirm the homogeneous distribution of nickel ferrite nanoparticles in the PVDF matrix.

3.7. Thermal stability analysis

Thermal degradation and the nucleation of the ferroelectric phases of PVDF can be significantly impacted by the geometrical factor such as size of the nanoparticles and the interaction at the interface between nanofillers and polymer. [38] We use thermogravimetric analysis (TGA) to study the thermal behavior of PVDF with the various amount of nickel ferrite loading. TGA thermograms and the corresponding differential TGA plots for various nickel ferrite nanoparticle loading, ranging from 0 to 30 wt%, are shown in Fig. 5. The typical one step thermal degradation characteristic of PVDF changes to two step degradation with 5 to 20 wt% loading, while an additional degradation step (identified as third step) is observed with 30 wt% loading. This third step is well identified in the derivative of the TGA curve (green line, Fig. 5b). These additional degradation steps in the presence of nanoparticles can be linked to the interaction between the polymer matrix and the nanoparticles.[15] Interestingly, loading of nickel ferrite nanoparticles significantly improved the thermal property of the PVDF film as evidenced by an 600% enhancement in thermal stability of PVDF film at 1000 °C with 30 wt% of nickel ferrite additive.

As shown in Fig. 5b, the first step of degradation of the polymer occurs between 440 and 500 °C, and the polymer maximum degradation temperature is affected by the percentage of loading of nanoparticle in the nanocomposite. In this first degradation step, the decomposition mechanism is related to chain-stripping where carbon-hydrogen and carbon–fluorine scission occurs and the presence of both hydrogen and fluorine radicals leads to the formation of hydrogen fluoride. [15,39].

3.8. Evidence of possible ferroelectric domains

The ferroelectric behavior and polarization domain structure were characterized by means of piezoresponse force microscopy (PFM) measurements in ambient environment.[40,41] The spatially resolved PFM imaging, performed on the pure PVDF and nanocomposite films, show that there is a sub-micron domain structure. Fig. 6a, 6b shows the respective amplitude and phase images of pure PVDF film where different phase contrasts indicate opposite out-of-plane polarization directions. The respective images for 5 %NiFe-PVDF nanocomposite are shown in Fig. 6d and 6e, where similar sized domains are observed.

The local polarization switching behaviors on the pure PVDF and 5 %NiFe-PVDF nanocomposite samples are characterized by the PFM switching spectroscopy method and the data are shown in Fig. 6c and Fig. 6f respectively, where PFM hysteresis loops (PFM signals as a function of applied dc bias) are obtained on the two samples, which is typical for these PVDF and PVDF copolymer ferroelectric films.[42]' [43].

The pure PVDF sample shows a negative piezoelectric coefficient from the PFM hysteresis loop measurement, i.e., a negative PFM signal for downward polarization at far positive voltage side (Fig. 6c). This negative piezoelectric behavior corresponds to sample contraction upon a positive PFM modulation voltage to the tip, while the 5 %NiFe-PVDF (Fig. 6f) shows a positive piezoelectric coefficient with an opposite PFM signal sign. Negative piezoelectric coefficients for PVDF are well established.[36,44].

Polarization switching of the pure PVDF and 5 %NiFe-PVDF nanocomposite samples takes place at the coercive voltages where the PFM signal reverses the sign. The coercive voltage is significant and typical of PVDF domains 300 nm thick or more.[42] Artifacts are not completely excluded, like charge trapping, and a ferroelectric Curie temperature was not established for these samples as the temperature of the paraelectric - ferroelectric phase transition in PVDF is above its melting temperature.[42].

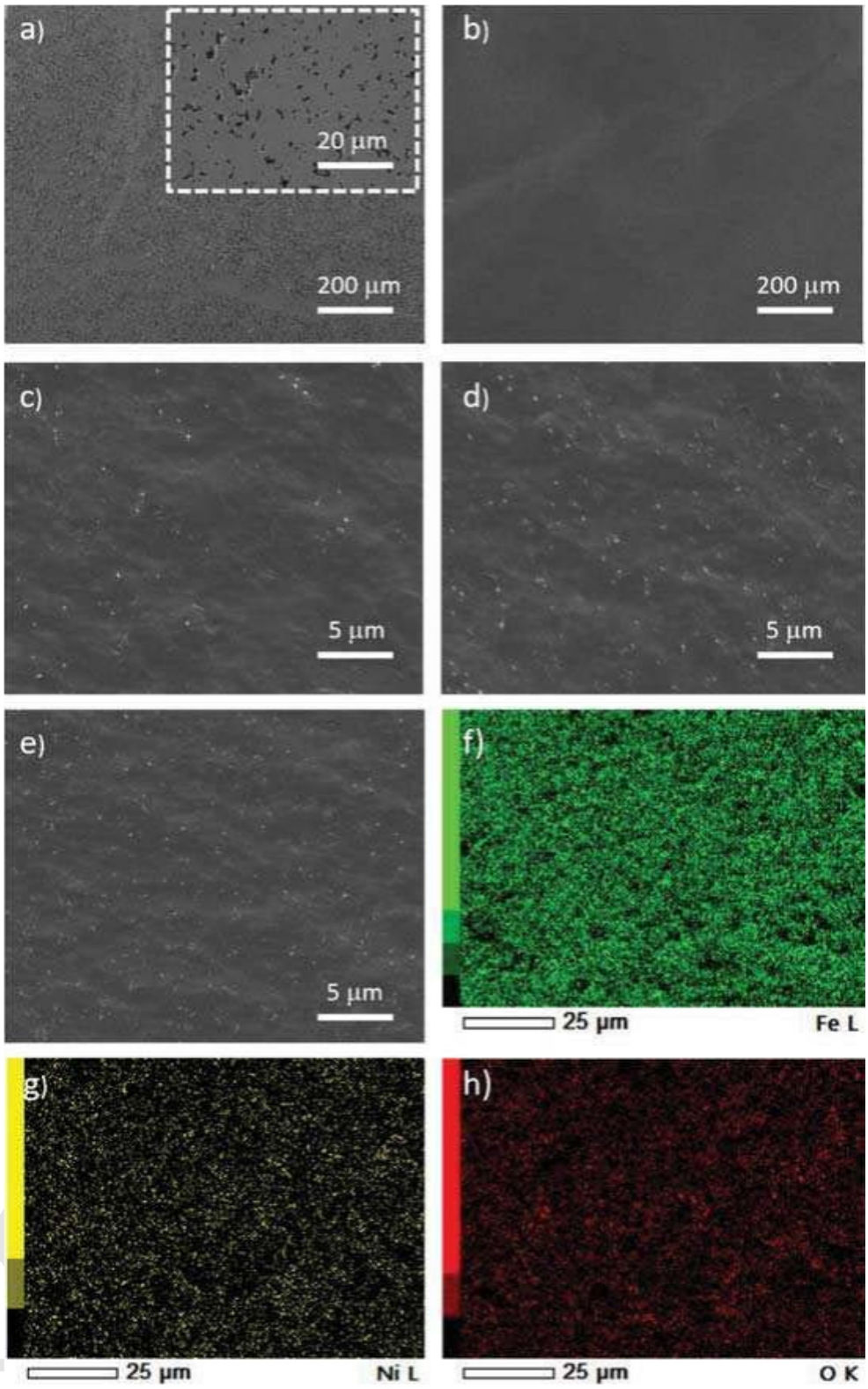

Fig. 4. FE-SEM micrographs of films: (a) Surface morphology of pure PVDF film at room temperature. Inset shows high-resolution image where voids due to phase separation can be seen. (b) Surface morphology of pure PVDF film at 95 °C. (c) Surface morphology of PVDF-5NF nanocomposite film at 95 °C. (d) Surface morphology of PVDF-10% nickel ferrite nanocomposite film at 95 °C. (e) Surface morphology of PVDF-20% nickel ferrite nanocomposite film at 95 °C. (f-h) EDX elemental mapping of PVDF-30% nickel ferrite nanocomposite film, showing uniform distribution of nickel ferrite nanoparticles in the PVDF matrix.

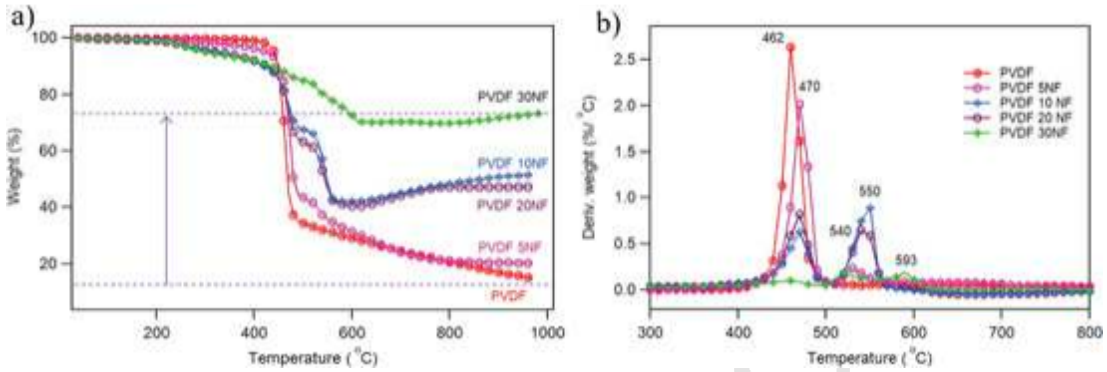

Fig. 5. Thermal behavior of PVDF film and a series of PVDF-nickel ferrite nanocomposite films. (a) TGA plots of pure PVDF and nanocomposite films. Nickel ferrite loading significantly improved the thermal stability of the PVDF, sowing 600 % increase in thermal stability at 1000 ^{O}C upon 30 wt% of NF loading. (b) Derivative thermogravimetric (DTG) curves of pure PVDF and nanocomposite films.

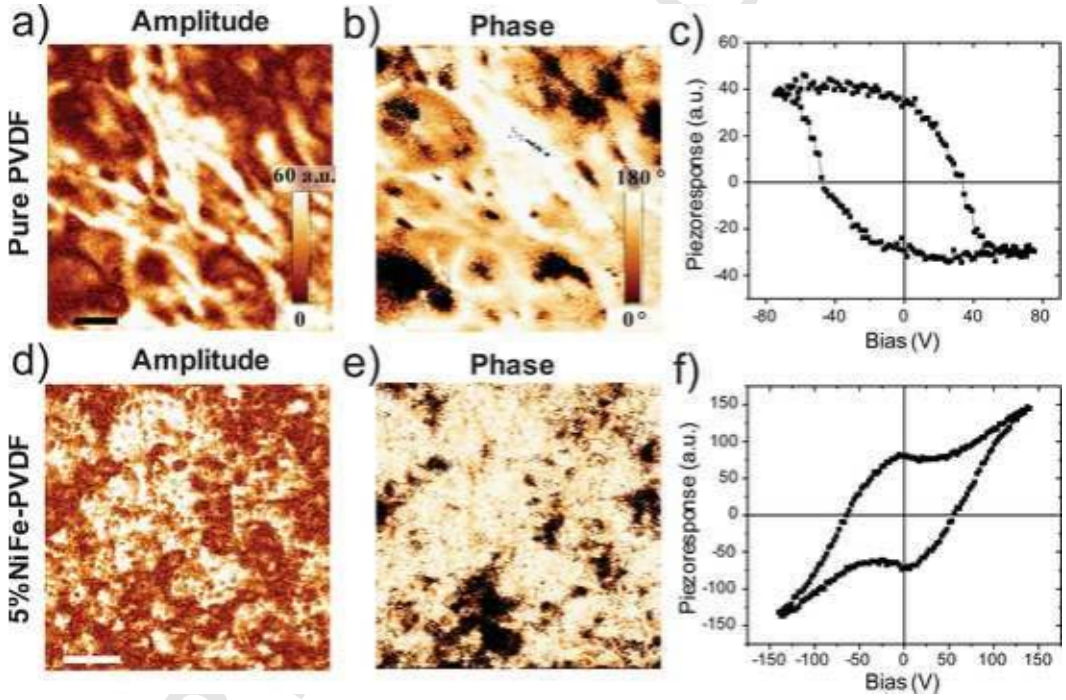

Fig. 6. Ferroelectric domain structures and polarization switching behaviors of pure PVDF (top panels, a-c) and 5 %NiFe-PVDF nanocomposites (bottom panels, d-f) characterized by piezoresponse force microscopy (PFM) techniques at room temperature: PFM amplitude (a, d), phase images (b, c), and PFM switching spectroscopy (c, f), respectively. The scale bars are 300 nm in (a) and (d).

3.9. Magnetic property studies

The magnetization properties of nickel ferrite nanoparticles and nanocomposite films were studied SQUID. The variation in the magnetization of nickel ferrite nanoparticles and PVDF-$NiFe_2O_4$ nanocomposite films as a function of the magnetic field, recorded at room temperature (300 K), is shown in Fig. 6a and Fig. 6b respectively. The magnetization of nickel ferrite nanoparticles at a magnetic field of 5 kOe is 37.3 emu/g. The magnetization value of our nickel ferrite nanoparticles is in agreement with earlier reports.[2,24,45,46] For the nanocomposite films, the magnetization (magnetic moment per unit gram) decreases, this behavior is expected due to the non-magnetic nature of PVDF material. The similar hysteresis loops of the nanocomposite films as of nickel ferrite are observed, which can be attributed to the uniform distribution of $NiFe_2O_4$ nanoparticles in the PVDF matrix. Magnetization at 5 kOe (M_{5kOe}), remanent magnetization (M_r), and coercivity (H_c) of nickel ferrite nanoparticles and nanocomposite films are listed in Table 1. The magnetization of the PVDF-NiFe2O4 nanocomposites increases with increasing $NiFe_2O_4$ filler content. The value of magnetization at 5 kOe as a function of nickel ferrite content is shown in the inset of Fig. 7a. The presence of a nonzero remanent magnetization is consistent with ferromagnetism. The magnetic properties of the $NiCo_2O_4$ (1 1 1) thin films have been studied systematically.[47,48] In particular, for the semiconducting $NiCo_2O_4$ (1 1 1) films, grown on Al_2O_3 (0 0 1) film, ferrimagnetism occurs below T_c = 330 K. Although the easy axis is not along the out-of-plane direction, there is significant remanence (>50% saturation value) with a coercivity about 1000 Oe.

Table 1
Magnetic parameters of the PVDF-$NiFe_2O_4$ films.

Sample	M_{5kOe} (emu/g)	M_r (emu/g)	H_c (Oe)
Nickel ferrite	37.3	2.29	27.9
PVDF-5 %NF	3.38	0.14	18.1
PVDF-10 %NF	6.96	0.28	19.3
PVDF-20 %NF	16.41	0.62	20.5
PVDF-30 %NF	23.85	0.85	21.2

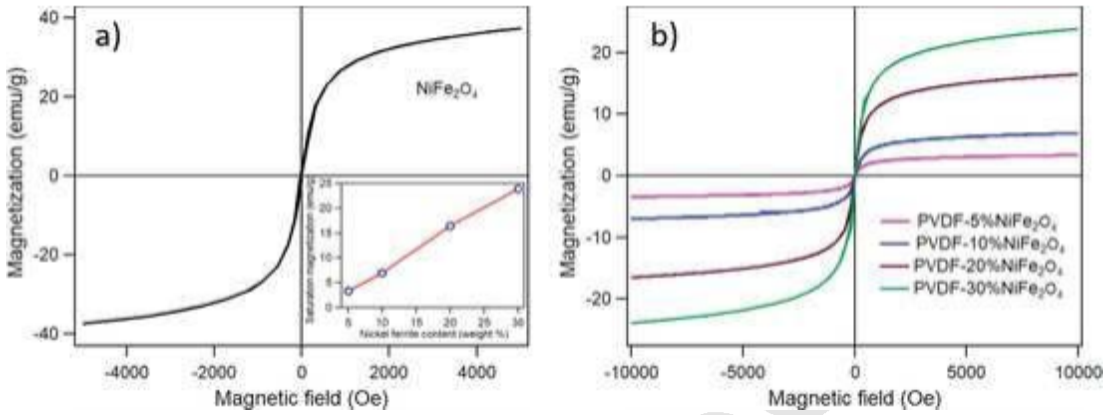

Fig. 7. Magnetic hysteresis loop of $NiFe_2O_4$ (a) and PVDF-$NiFe_2O_4$ nanocomposite films (b). Inset shows the variation of magnetization at 5 kOe as a function of $NiFe_2O_4$ loading.

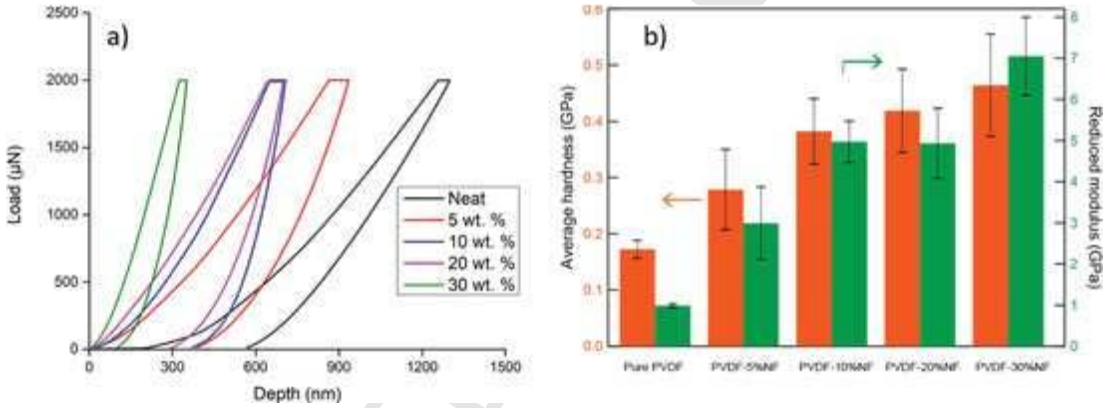

Fig. 8. (a) Nanoindentation load–displacement curves of pure PVDF and various wt% of nickel ferrite incorporated PVDF-nickel ferrite nanocomposites. (b) Average hardness (left axis) and average reduced modulus (right axis) of pure PVDF and various wt% of nickel ferrite incorporated PVDF-nickel ferrite nanocomposites. Error bars denote statistical reproducibility for all measurements.

[47] Here the coercivity and remanent magnetization is much smaller than seen for $NiFe_2O_4$ thin films, consistent with the nanoparticle morphology of the $NiFe_2O_4$ in PVDF matrix. For nanoparticles of the $NiFe_2O_4$ in PVDF matrix, few particles will be aligned with the easy axis parallel to the applied magnetic field, so true magnetic saturation requires large applied fields and thus is elusive, as seen here (Fig. 7). (SeeFig. 8.).

3.10. Nanoindentation

Nanoindentation was performed to characterize the nanomechanical properties of pure PVDF and PVDF-NiFe2O4 nanocomposite films. For nanoindentation experiments, thin film samples were carefully mounted on to the AFM pucks and the indentation tests were conducted in load control mode. For load control mode, the indentation includes a constant loading, unloading rate, and a holding segment at maximum load. A maximum load of 2000 μN was applied with a dwell time (hold time) of 5 sec and loading/unloading rate of 400 μN/s. The indentation depth was kept small compared to the total material thickness so that the substrate effect on determining the mechanical property of the material could be avoided.

To estimate nanomechanical characteristics, a test sample was indented or loaded by an intender tip and then unloaded, and the load–displacement data were recorded (see Fig. 7a). Load-displacement data were then analyzed using a common method to determine hardness and elastic modulus of films. The average hardness of pure PVDF and PVDF-nickel ferrite nanocomposite films is shown in Fig. 7b (left axis). With the increase in content of nickel ferrite nanoparticles in the PVDF matrix, the average hardness value is found to be increased. The average hardness value for 30 %NiFe-PVDF film (0.47 GPa) is found to be a 3 times higher than the pure PVDF film (0.16 GPa). This suggests that the incorporation of nickel ferrite has favorable effect on the hardness of the film. Similarly, the average reduced modulus value is found to increase with the increase in the content of nickel ferrite nanoparticles in the PVDF matrix (Fig. 7b (right axis)). The maximum reduced modulus is found to be 7.1 GPa with 30 %NiFe-PVDF film, which is seven times higher than the pure PVDF film (0.98 GPa).

4. Conclusions

We report a straightforward sonochemical method to prepare nickel ferrite nanoparticles of average diameter 18 ± 3.7 nm. As-synthesized nickel ferrite nanoparticles are highly crystalline in nature and demonstrated the cubic spinel structure with good magnetic properties. Next, we fabricated pure PVDF and nanocomposite films by incorporating various weight percentage of as-synthesized nanoparticles in PVDF matrix using a blade coating technique. By optimizing the processing parameters of the coating, we obtain highly smooth, good optical quality, and void-free flexible films. XRD and FTIR analysis confirmed the presence of predominant ferroelectric β-crystalline phase in pure PVDF and nanocomposite films. Microstructure analysis showed the homogeneous distribution of nickel ferrite nanoparticles in the PVDF matrix. Further, the investigation of effect of nickel ferrite nanoparticles on thermal degradation of PVDF demonstrated a 600 % increase in thermal stability of PVDF film at 1000 °C with the infusion of 30 wt% of nickel ferrite nanoparticles. Magnetic measurements confirm the ferro-

magnetic nature of nanocomposite films at room temperature. We also present evidence of sub-microns sized ferroelectric domain structure and switching of domains by polling with dc bias. The pure PVDF film demonstrated a negative piezoelectric coefficient from the PFM hysteresis loop measurement whereas the 5% nickel ferrite-PVDF nanocomposite showed a positive piezoelectric coefficient. The nanoindentation tests revealed 3-fold and 7-fold enhancement in average hardness and reduced modulus with the 30 %NiFe-PVDF film than pure PVDF film. Finally, the achievement of smooth, pin-hole free, ultra-thin films of PVDF and nanocomposites could be suitable candidate for the development capacitor devices.

Data availability

The data supporting the finding of the study are available within the article or from the corresponding author upon request.

Declaration of Competing Interest

The authors declare that they have no known competing financial interests or personal relationships that could have appeared to influence the work reported in this paper.

Acknowledgments

We thank Farooq Syed for his assistance with nanoindentation experiment. This research work was supported from the National Science Foundation (NSF-PREM # 1827690) and the Nebraska MRSEC (DMR-1420645). We thank Professor Peter Dowben for his comments on this paper.

References:

[1] R.J. Klein, J. Runt, Q. Zhang, Influence of crystallization conditions on the microstructure and electromechanical properties of poly (vinylidene fluoride–trifluoroethylene– chlorofluoroethylene) terpolymers, Macromolecules 36 (19) (2003) 7220–7226.

[2] A. Mayeen, K. M. s., J. M. s., S. Thomas, J. Philip, D. Rouxel, R.N. Bhowmik, N. Kalarikkal, Flexible and self-standing nickel ferrite–PVDF-TrFE cast films: promising candidates for high-end magnetoelectric applications, Dalton Trans. 48 (45) (2019) 16961–16973.

[3] M. Silva, S. Reis, C.S. Lehmann, P. Martins, S. Lanceros-Mendez, A. Lasheras, J. Gutiérrez, J.M. Barandiarán, Optimization of the magnetoelectric response of poly (vinylidene fluoride)/epoxy/vitrovac laminates, ACS Appl. Mater. Interfaces 5 (21) (2013) 10912–10919.

[4] P. Martins, Y.V. Kolen'ko, J. Rivas, S. Lanceros-Mendez, Tailored magnetic and magnetoelectric responses of polymer-based composites, ACS Appl. Mater. Interfaces 7 (27) (2015) 15017–15022.

[5] V.S.D. Voet, M. Tichelaar, S. Tanase, M.C. Mittelmeijer-Hazeleger, G. ten Brinke, K. Loos, Poly (vinylidene fluoride)/nickel nanocomposites from semicrystalline block copolymer precursors, Nanoscale 5 (1) (2013) 184–192.

[6] S.-W. Cheong, M. Mostovoy, Multiferroics: a magnetic twist for ferroelectricity, Nat. Mater. 6 (1) (2007) 13–20.

[7] W. Eerenstein, N. Mathur, J.F. Scott, Multiferroic and magnetoelectric materials, Nature 442 (7104) (2006) 759–765.

[8] N.A. Spaldin, M. Fiebig, The renaissance of magnetoelectric multiferroics, Science 309 (5733) (2005) 391–392.

[9] M. Fiebig, T. Lottermoser, D. Meier, M. Trassin, The evolution of multiferroics, Nat. Rev. Mater. 1 (8) (2016).

[10] Onuta, T.-D., et al., *Energy harvesting properties of all-thin-film multiferroic cantilevers.* Applied Physics Letters, 2011. **99**(20): p. 203506.

[11] N.A. Spaldin, R. Ramesh, Advances in magnetoelectric multiferroics, Nat. Mater. 18 (3) (2019) 203–212.

[12] A. Omelyanchik, V. Antipova, C. Gritsenko, V. Kolesnikova, D. Murzin, Y. Han, A.V. Turutin, I.V. Kubasov, A.M. Kislyuk, T.S. Ilina, D.A. Kiselev, M.I. Voronova, M.D. Malinkovich, Y.N. Parkhomenko, M. Silibin, E.N. Kozlova, D. Peddis, K. Levada, L. Makarova, A. Amirov, V. Rodionova, Boosting Magnetoelectric effect in polymer-based nanocomposites, Nanomaterials 11 (5) (2021) 1154.

[13] Nan, C.-W., et al., *Large magnetoelectric response in multiferroic polymer-based composites.* Physical Review B, 2005. **71**(1): p. 014102.

[14] X. Cai, T. Lei, D. Sun, L. Lin, A critical analysis of the α, β and γ phases in poly (vinylidene fluoride) using FTIR, RSC Adv. 7 (25) (2017) 15382–15389.

[15] P. Martins, C.M. Costa, M. Benelmekki, G. Botelho, S. Lanceros-Méndez, Interface characterization and thermal degradation of ferrite/poly (vinylidene fluoride) multiferroic nanocomposites, J. Mater. Sci. 48 (6) (2013) 2681–2689.

[16] A. Jain, P. K. j., A.K. Sharma, A. Jain, R. P.n, Dielectric and piezoelectric properties of PVDF/PZT composites: a review, Polym. Eng. Sci. 55 (7) (2015) 1589–1616.

[17] A.J. Lovinger, Recent developments in the structure, properties, and applications of ferroelectric polymers, Jpn. J. Appl. Phys. 24 (S2) (1985) 18.

[18] W. Xia, Z. Zhang, PVDF-based dielectric polymers and their applications in electronic materials, Iet. Nanodielectrics 1 (1) (2018) 17–31.

[19] S. Garain, T.K. Sinha, P. Adhikary, K. Henkel, S. Sen, S. Ram, C. Sinha, D. Schmeißer, D. Mandal, Self-poled transparent and flexible UV light-emitting cerium complex–PVDF composite: a high-performance nanogenerator, ACS Appl. Mater. Interfaces 7 (2) (2015) 1298–1307.

[20] S. Sarkar, S. Garain, D. Mandal, K.K. Chattopadhyay, Electro-active phase formation in PVDF–BiVO 4 flexible nanocomposite films for high energy density storage application, RSC Adv. 4 (89) (2014) 48220–48227.

[21] A. Kumar, K. Yadav, Enhanced magnetocapacitance sensitivity in BiFeO3–poly (vinylidene-fluoride) hot pressed composite films, J. Alloy. Compd. 528 (2012) 16–19.

[22] P. Martins, C.M. Costa, G. Botelho, S. Lanceros-Mendez, J.M. Barandiaran, J. Gutierrez, Dielectric and magnetic properties of ferrite/poly (vinylidene fluoride) nanocomposites, Mater. Chem. Phys. 131 (3) (2012) 698–705.

[23] C. Behera, R. Choudhary, P.R. Das, Development of multiferroism in PVDF with CoFe 2 O 4 nanoparticles, J. Polym. Res. 24 (4) (2017) 56.

[24] T. Prabhakaran, J. Hemalatha, Magnetoelectric investigations on poly (vinylidene fluoride)/NiFe 2 O 4 flexible films fabricated through a solution casting method, RSC Adv. 6 (90) (2016) 86880–86888.

[25] C. Behera, R. Choudhary, P.R. Das, Development of Ni-ferrite-based PVDF nanomultiferroics, J. Electron. Mater. 46 (10) (2017) 6009–6022.

[26] B. Sapkota, et al., High permeability sub-nanometre sieve composite MoS 2 membranes, Nat. Commun. 11 (1) (2020) 1–9.

[27] D.K. Rana, S.K. Singh, S.K. Kundu, S. Roy, S. Angappane, S. Basu, Electrical and room temperature multiferroic properties of polyvinylidene fluoride nanocomposites doped with nickel ferrite nanoparticles, New J. Chem. 43 (7) (2019) 3128–3138.

[28] M.N. Zafar, Q. Dar, F. Nawaz, M.N. Zafar, M. Iqbal, M.F. Nazar, Effective adsorptive removal of azo dyes over spherical ZnO nanoparticles, J. Mater. Res. Technol. 8 (1) (2019) 713–725.

[29] S.R. Mishra, H. Adhikari, D.L. Kunwar, C. Ranaweera, B. Sapkota, M. Ghimire, R. Gupta, J. Alam, Facile hydrothermal synthesis of hollow Fe3O4 nanospheres: effect of hydrolyzing agents and electrolytes on electrocapacitive performance of advanced electrodes, Int. J. Metall Met. Phys. 2 (1) (2017) 1–15.

[30] W. Armstrong, B. Sapkota, S.R. Mishra, Silver decorated carbon nanospheres as effective visible light photocatalyst, MRS Online Proceedings Library (OPL) 1509 (2013).

[31] D. Neupane, H. Adhikari, B. Sapkota, J. Candler, R. Gupta, S.R. Mishra, Surfactant assisted synthesis of SrFe 10 Al 2 O 19: magnetic and Supercapacitor ferrite, MRS Adv. 1 (45) (2016) 3099–3106.

[32] Sapkota, B.B. and S.R. Mishra, *Preparation and Photocatalytic Activity Study of p-CuO/n-ZnO Nanocomposites.*

[33] K. Maaz, S. Karim, A. Mumtaz, S.K. Hasanain, J. Liu, J.L. Duan, Synthesis and magnetic characterization of nickel ferrite nanoparticles prepared by co-precipitation route, J. Magn. Magn. Mater. 321 (12) (2009) 1838–1842.

[34] U. Valiyaneerilakkal, A. Singh, C.K. Subash, K. Singh, S.M. Abbas, S. Varghese, Preparation and characterization of poly (vinylidene fluoride-trifluoroethylene)/barium titanate polymer nanocomposite for ferroelectric applications, Polym. Compos. 38 (8) (2017) 1655–1661.

[35] M. Neidhöfer, F. Beaume, L. Ibos, A. Bernès, C. Lacabanne, Structural evolution of PVDF during storage or annealing, Polymer 45 (5) (2004) 1679–1688.

[36] I. Katsouras, K. Asadi, M. Li, T.B. van Driel, K.S. Kjær, D. Zhao, T. Lenz, Y. Gu, P.W.M. Blom, D. Damjanovic, M.M. Nielsen, D.M. de Leeuw, The negative piezoelectric effect of the ferroelectric polymer poly (vinylidene fluoride), Nat. Mater. 15 (1) (2016) 78–84.

[37] A. Gupta, R.P. Tandon, *Organic–inorganic hybrid polyvinylidene fluoride–Co 0.6 Zn 0.4 Mn 0.3 Fe 1.7 O 4 nanocomposite film with significant optical and magnetodielectric properties.* RSC, Advances 5 (14) (2015) 10110–10118.

[38] S. Jiao, Z. Sun, Y. Zhou, F. in J. Wen, Y. Chen, X. Du, L. in Y. Liu, Surface-coated thermally expandable microspheres with a composite of polydisperse graphene oxide sheets, Surface-Coated Thermally Expandable Microspheres with a Composite of Polydisperse Graphene Oxide Sheets. 14 (23) (2019) 4328–4336.

[39] G. Botelho, S. Lanceros-Mendez, A.M. Gonçalves, V. Sencadas, J.G. Rocha, Relationship between processing conditions, defects and thermal degradation of poly (vinylidene fluoride) in the β-phase, J. Non-Cryst. Solids 354 (1) (2008) 72–78.

[40] Z. Zhang, R. González, G. Díaz, L.G. Rosa, I. Ketsman, X. Zhang, P. Sharma, A. Gruverman, P.A. Dowben, Polarization mediated chemistry on ferroelectric polymer surfaces, J. Phys. Chem. C 115 (26) (2011) 13041–13046.

[41] A. Gruverman, O. Auciello, H. Tokumoto, Imaging and control of domain structures in ferroelectric thin films via scanning force microscopy, Annu. Rev. Mater. Sci. 28 (1) (1998) 101–123.

[42] L.M. Blinov, V.M. Fridkin, S.P. Palto, A.V. Bune, P.A. Dowben, S. Ducharme, Two-dimensional ferroelectrics, Phys. Usp. 43 (3) (2000) 243–257.

[43] F. Wong, G. Perez, M. Bonilla, J.A. Colon-Santana, X. Zhang, P. Sharma, A. Gruverman, P.A. Dowben, L.G. Rosa, Changing molecular band offsets in polymer blends of (P3HT/P (VDF–TrFE)) poly (3-hexylthiophene) and poly (vinylidene fluoride with trifluoroethylene) due to ferroelectric poling, RSC Adv. 4 (6) (2014) 3020–3027.

[44] L.u. You, Y. Zhang, S. Zhou, A. Chaturvedi, S.A. Morris, F. Liu, L. Chang, D. Ichinose, H. Funakubo, W. Hu, T. Wu, Z. Liu, S. Dong, J. Wang, Origin of giant negative piezoelectricity in a layered van der Waals ferroelectric, Sci. Adv. 5 (4) (2019).

[45] G.D. Prasanna, R.L. Ashok, V.B. Prasad, H.S. Jayanna, Synthesis and characterization of magnetic and conductive nickel ferrite–polyaniline nanocomposites, J. Compos. Mater. 49 (21) (2015) 2649–2657.
[46] J. Jiang, Y.-M. Yang, Facile synthesis of nanocrystalline spinel NiFe2O4 via a novel soft chemistry route, Mater. Lett. 61 (21) (2007) 4276–4279.
[47] Zhen, C., et al., *Nanostructural origin of semiconductivity and large magnetoresistance in epitaxial NiCo2O4/Al2O3 thin films.* Journal of Physics D: Applied Physics, 2018. **51**(14): p. 145308.
[48] C. Mellinger, et al., Perpendicular magnetic anisotropy in conducting NiCo 2 O 4 films from spin-lattice coupling, Phys. Rev. B 101 (1) (2020) 014413.